J Biol Inorg Chem (2013) 18:791–801
DOI 10.1007/s00775-013-1022-4

ORIGINAL PAPER

Study of the synthesis, antiproliferative properties, and interaction with DNA and polynucleotides of cisplatin-like Pt(II) complexes containing carcinogenic polyaromatic amines

Elisabetta Gabano · Sofia Gama · Filipa Mendes · Marzia B. Gariboldi · Elena Monti · Sophie Bombard · Sabrina Bianco · Mauro Ravera

Received: 21 March 2013 / Accepted: 30 June 2013 / Published online: 20 July 2013
© SBIC 2013

Abstract The chemical and biological features of two newly synthesized [$PtCl_2$(L)(2-aminonaphthalene)] complexes (L is NH_3 or 2-aminonaphthalene) were compared with those of two already reported enantiomeric complexes of formula [$PtCl_2$(DABN)] [DABN is (*R*)-1,1′-binaphthyl-2,2′-diamine or (*S*)-1,1′-binaphthyl-2,2′-diamine]. Solution behavior, lipophilicity, cytotoxicity with regard to one colorectal (HCT116) and two ovarian (A2780 and A2780Cp8) human carcinoma cell lines, and in vitro DNA- and G-quadruplex-binding properties were evaluated. In particular, the cytotoxicity of [$PtCl_2(NH_3)$(2-aminonaphthalene)] was better than that of cisplatin for all cell lines, and rather resembled that of oxaliplatin. The solution behavior of the whole series of complexes and the absence of an evident relationship between lipophilicity and cytotoxicity seem to suggest that all these experimental parameters are probably smoothed out during the 3-day cytotoxicity experiments and do not strongly affect the half-maximal inhibitory concentrations. The results of electrophoretic studies indicate that different kinds of interaction with DNA can be involved in the mode of action of these complexes, with intercalation in double-stranded DNA and stacking on G-quadruplex DNA being strongly implicated in particular for [$PtCl_2(NH_3)$(2-aminonaphthalene)].

Keywords Platinum complexes · DNA interaction · Cytotoxicity

Electronic supplementary material The online version of this article (doi:10.1007/s00775-013-1022-4) contains supplementary material, which is available to authorized users.

E. Gabano · S. Bianco · M. Ravera (✉)
Dipartimento di Scienze e Innovazione Tecnologica (DiSIT), Università del Piemonte Orientale "Amedeo Avogadro", Viale Michel 11, 15121 Alessandria, Italy
e-mail: mauro.ravera@unipmn.it

S. Gama · F. Mendes
Unidade de Ciências Químicas e Radiofarmacêuticas, Instituto Superior Técnico-Campus Tecnológico e Nuclear, Estrada Nacional 10 (km 139,7), 2695-066 Bobadela LRS, Portugal

M. B. Gariboldi · E. Monti
Dipartimento di Scienze Teoriche e Applicate (DiSTA), Università dell'Insubria, Via H. Dunant 3, 21100 Varese, Italy

S. Bombard
Université Paris Descartes, INSERM UMR-S-1007, 45 rue des Saints-Pères, 75006 Paris, France

Introduction

Direct interaction with DNA is recognized as a major mechanism for the antitumor effect of a number of low molecular weight compounds [1]. In this regard, the discovery of the antitumor properties of cisplatin—*cis*-diamminedichloridoplatinum(II), [$PtCl_2(NH_3)_2$]—probably represents a milestone that has led to extensive investigation of the interactions between metal complexes and biomolecules [2].

Interaction between metal complexes and oligonucleotides may occur through (1) external electrostatic binding between cationic complexes and the anionic phosphate groups of the DNA backbone, (2) intercalation between stacked base pairs in the double helix structure (in particular, in the presence of ligands with planar aromatic substituents, an ensemble of weak noncovalent interactions between the ligands and the nucleic acids may occur [3, 4]), (3) stacking on guanine quadruplex (G-quadruplex) structures [5], and (4) covalent bonds between the Lewis acidic metal and nucleic acid Lewis bases (in particular, N7

of adenine and guanine residues, albeit N7 of guanine shows a greater kinetic preference) [6].

The commonest covalent Pt–DNA adducts of cisplatin derivatives are intrastrand cross-links between neighboring purine bases (1,2-GG or 1,2-AG intrastrand cross-links), intrastrand cross-links between purine bases separated by a third base, and interstrand cross-links; monofunctional adducts can also be formed. The resulting changes in the DNA structure interfere with cellular processes, leading to cell death [6]. Removal of Pt–DNA adducts by DNA repair mechanisms can restore the integrity of the genome, causing resistance to platinum-based chemotherapy. For this reason, complexes able to interact with DNA in a way different from that of cisplatin may represent a method to overcome acquired platinum resistance [7].

More recently, platinum complexes have also been proposed as drugs able to target telomeric DNA [8]. Telomeres are nucleoprotein complexes consisting of guanine-rich repeats of DNA [$(TTAGGG)_n$ in humans] protecting the end of linear chromosomes [9]. The guanine-rich strand can adopt a variety of unusual DNA conformations, but only G-quadruplex DNA and T-loops are stable in vitro under physiological conditions. The former four-stranded structure consists of four stacked quartets of guanine bases (G-quartets) hydrogen-bonded by Hoogsteen base pairing [10, 11]. In normal cells, telomeres shorten by 50–200 base pairs for each round of replication because of the incomplete replication of the 5′ end of the lagging DNA strand [12]; telomere shortening below a critical length leads to senescence and/or apoptosis, unless new telomeric repeats are added by telomerase. This enzyme is usually inactivated in differentiated cells, but it is reactivated in approximately 85–90 % of human tumors, thus conferring unlimited replicative potential and contributing to the malignant transformation. For these reasons, molecules able to inhibit the action of telomerase (directly or through stabilization of G-quadruplexes) might selectively induce cancer cell death [13]. Indeed, not only were some small molecules that can specifically stabilize G-quadruplex in vitro able to inhibit telomerase activity in cells [14], but some of them were also shown to induce cell death through the displacement of protective telomeric protein components [15, 16], as well as by perturbing the function of some of the genes containing G-quadruplex motifs [17].

In this study, two [$PtCl_2$(L)(**L1**)] complexes (L is NH_3 and **L1** is 2-aminonaphthalene—**PtL1**; L and **L1** are 2-aminonaphthalene—**Pt(L1)$_2$**; Fig. 1) were tested for their cytotoxicity (with regard to ovarian A2780 and A2780Cp8 and colon HCT116 cells) and their ability to interact with supercoiled DNA and G-quadruplexes. Their behavior was compared with that of two enantiomeric complexes with formulas [$PtCl_2$(*R*)-DABN] (**PtL2**) and [$PtCl_2$(*S*)-DABN]

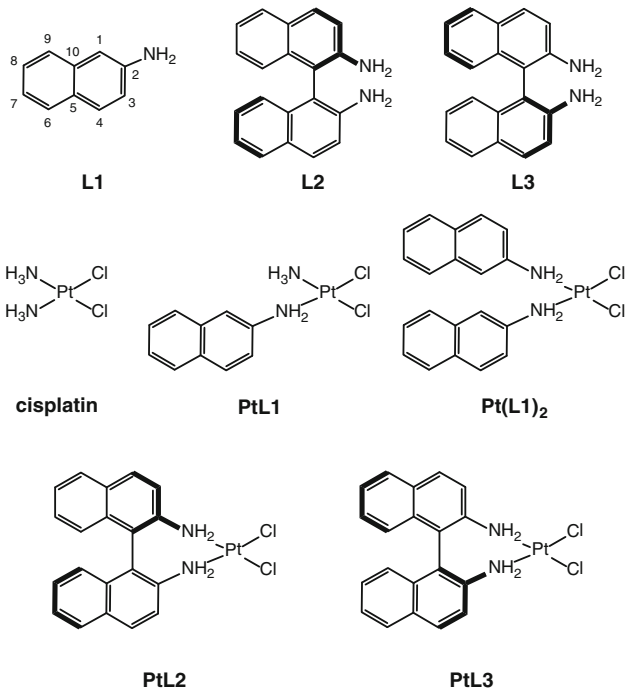

Fig. 1 The ligands and their platinum complexes investigated

(**PtL3**) bearing 1,1′-binaphthyl-2,2′-diamine (DABN) ligands. The aim of this work is to evaluate the effect of different combination of ligands (i.e., a single 2-aminonaphthalene and two nonlinked 2-aminonaphthalenes vs DABN, which can be regarded as two linked 2-aminonaphthalenes) on the biological behavior of the corresponding complexes. The cytotoxicity and G-quadruplex-binding properties of **PtL2** and **PtL3** have been described in a previous article [18].

Materials and methods

General

All chemicals (analytical grade) were obtained from Aldrich, except K_2PtCl_4 (Alfa Aesar), and were used as received. $K[PtCl_3NH_3]$, prepared according to procedures described in the literature [19–21], was reacted with 2-aminonaphthalene in methanol to give **PtL1**. **Pt(L1)$_2$** was prepared via the reaction of $K_2[PtCl_4]$ and 2-aminonaphthalene in a mixture of methanol and water [22] (see later for experimental details).

Elemental analyses were conducted with an EA3000 CHN elemental analyzer (EuroVector, Milan, Italy) and completed with the determination of the platinum content. The latter was quantified by means of a Spectro Genesis inductively coupled plasma optical emission spectroscopy spectrometer (Spectro Analytical Instruments, Kleve,

Germany) equipped with a cross-flow nebulizer. A platinum standard stock solution of 1,000 mg L^{-1} was diluted in 1.0 % v/v nitric acid to prepare calibration standards, and the platinum 299.797-nm line was selected for the measurement.

Multinuclear NMR spectra were measured with a JEOL Eclipse Plus instrument operating at 400 MHz (^{1}H), 100.5 MHz (^{13}C), and 85.9 MHz (^{195}Pt), respectively. ^{1}H and ^{13}C NMR chemical shifts were reported in parts per million referenced to solvent resonances. ^{195}Pt NMR spectra were recorded using a solution of K_2PtCl_4 in saturated aqueous KCl as the external reference. The shift for $K_2[PtCl_4]$ was adjusted to −1,628 ppm relative to $Na_2[PtCl_6]$ ($\delta = 0$ ppm).

Reversed-phase high-performance liquid chromatography (HPLC) and mass analysis were performed using a Waters HPLC–mass spectrometry (MS) instrument equipped with an Alliance 2695 separations module, 2487 dual lambda absorbance detector, and 3100 mass detector (see later for experimental details).

Synthesis of **PtL1**

$K[PtCl_3NH_3]$ (172 mg, 0,48 mmol) was dissolved in 5 mL water in the dark. 2-Aminonaphthalene (66 mg, 0.46 mmol) was dissolved in methanol (10 mL) and this solution was added dropwise to the former orange solution. The reaction mixture was stirred overnight at room temperature in the dark, was then cooled to complete the precipitation of the product, and was then centrifuged to isolate the yellow precipitate. The product was washed with cold water, a mixture of methanol and diethyl ether (10:90), and diethyl ether. Yield: 139 mg (68 %). Electrospray ionization MS (methanol) *m/z*: 449.02 $[M + Na]^+$; calcd for $C_{10}H_{12}Cl_2N_2NaPt$: 449.19 *m/z*. Anal. Calcd for $C_{10}H_{12}Cl_2N_2Pt$ (%): C, 28.18; H, 2.84; N, 6.57; Pt, 45.77. Found (%): C, 27.95; H, 2.55; N, 6.29; Pt, 45.63. ^{1}H NMR (methanol-d_4) δ (ppm): 7.87 (d, $^{3}J = 8.8$ Hz, 1H, H_4), 7.86-7.80 (m, 2H, H_6 and H_9), 7.70 (d, $^{4}J = 2.2$ Hz, 1H, H_1), 7.54 (dd, $^{3}J = 8.8$ Hz, $^{4}J = 2.2$ Hz, 1H, H_3), 7.47 (m, 2H, H_7 and H_8). ^{13}C{^{1}H} NMR (dimethylformamide-d_7) δ (ppm): 141.0 (C_2), 133.9 (C_{10}), 131.4 (C_5), 128.9 (C_3), 128.0 (C_1), 127.5 (C_4), 126.7 (C_6 or C_9), 125.4 (C_7 or C_8), 122.4 (C_7 or C_8), 118.3 (C_6 or C_9). ^{195}Pt NMR (methanol-d_4) δ (ppm): −2,123.

Synthesis of **Pt(L1)$_2$**

$K_2[PtCl_4]$ (195 mg, 0.47 mmol) was dissolved in 5 mL water in the dark and 2 mL methanol was added. 2-Aminonaphthalene (128 mg, 0.89 mmol) was dissolved in methanol (10 mL) and 2 mL water was added. This latter solution was added dropwise to the bright red solution of the platinum complex. The reaction mixture was stirred overnight at room temperature, and then the yellow precipitate was collected by centrifugation and washed with cold water, a mixture of methanol and diethyl ether (10:90), and diethyl ether, and dried under a vacuum. Yield: 160 mg (65 %). Electrospray ionization MS (methanol plus 0.1 % dimethylformamide) *m/z*: 575.03 $[M + Na]^+$; calcd for $C_{20}H_{18}Cl_2N_2NaPt$: 575.34 *m/z*. Anal. Calcd for $C_{10}H_{12}Cl_2N_2Pt$ (%): C, 43.49; H, 3.28; N, 5.07; Pt, 35.32. Found (%):C, 43.74; H, 2.99; N, 5.27; Pt, 35.42. ^{1}H NMR (dimethylformamide-d_7) δ (ppm): 7.84 (2H, m, H_6 or H_9), 7.76 (2H, d, $^{3}J = 9.15$ Hz, H_4), 7.71 (2H, s, H_1), 7.59 (4H, m, H_3 and H_9 or H_6), 7.45 (4H, m, H_7 and H_8). ^{13}C{^{1}H} NMR (dimethylformamide-d_7) δ (ppm): 140.31 (C_2), 133.42 (C_{10}), 131.42 (C_5), 128.52 (C_3), 127.81 (C_1), 127.35 (C_4), 126.63 (C_6 or C_9), 125.53 (C_8 or C_7), 123.02 (C_7 or C_8), 119.63 (C_6 or C_9). ^{195}Pt NMR (dimethylformamide-d_7) δ (ppm): −2,057.

Lipophilicity

Chromatographic analysis was used to evaluate the lipophilicity of the compounds. The chromatographic conditions were as follows [23, 24]: silica-based C_{18} gel as the stationary phase (5-μm Gemini® C_{18} column 25 mm × 3-mm inner diameter); 80:20 methanol/15 mM formic acid as the eluent (flow rate 0.5 mL/min; isocratic elution, UV–visible detector set at 210 nm). KCl was the internal reference to determine the column dead time (t_0). The concentrations of the platinum complex solutions were 0.1 mM. The retention time t_R in the actual experimental conditions was used to calculate $\log k'_{80}$ ($k'_{80} = (t_R - t_0)/t_0$).

Solution behavior

Solutions of **PtL1**, **PtL2**, and **PtL3** (1 mM) and **Pt(L1)$_2$** (0.1 mM) were prepared in water containing 35 % v/v ethanol (**PtL1**, **PtL2**, or **PtL3**) or 60 % v/v ethanol [**Pt(L1)$_2$**], incubated at 37 °C, and analyzed at regular time intervals via HPLC–MS. Reversed-phase HPLC and mass analysis were performed using a Waters HPLC–MS instrument equipped with an Alliance 2695 separations module, 2487 dual lambda absorbance detector, and 3100 mass detector. The chromatographic conditions were as follows [24]: silica-based C_{18} gel as the stationary phase (5-μm Gemini® C_{18} column 25 mm × 3-mm inner diameter); mobile phase containing 80:20 methanol/15 mM formic acid (flow rate 0.5 mL/min; isocratic elution, UV–visible detector set at 210 nm). KCl was the internal reference to determine the column dead time. The source and desolvation temperatures were set to 150 and 250 °C, respectively, with nitrogen used both as a drying gas and as

a nebulizing gas. The cone and the capillary voltages were usually 30 V and 2.70 kV, respectively. Quasi-molecular ion peaks $[M + H]^+$, sodiated $[M + Na]^+$ peaks, or the peaks of the aquated species $[M - Cl + H_2O]^+$ were assigned on the basis of the *m*/*z* values and the simulated isotope distribution patterns.

Cytotoxicity tests

Three human tumor cell lines were used for the present study: A2780 (ovarian carcinoma) and HCT116 (colon adenocarcinoma) cells were obtained from ATCC (Manassas, VA, USA); A2780Cp8 cells (so called because of their ability to grow in medium containing 8 μM cisplatin) were developed by chronic exposure of the parent cisplatin-sensitive cell line to increasing concentrations of cisplatin, and were obtained from Robert Ozols (Fox Chase Cancer Center, Philadelphia, PA, USA). A2780Cp8 cells differ from the parental cell line in a number of features that contribute to the resistant phenotype, including alterations in mismatch and nucleotide excision DNA repair systems and increased glutathione levels. HCT116 cells harbor a mutation in the *MLH1* gene [25], leading to defective mismatch repair activity [26]. Deficits in mismatch repair are known to impair tumor response to cisplatin, whereas response to oxaliplatin—*cis*-[(1*R*,2*R*)-cyclohexanediamine]oxalatoplatinum(II)—is unaffected, and are fairly common in colorectal cancer, partially explaining why the latter is effective in this cancer type whereas the former generally is not [27]. The three cell lines were maintained in RPMI 1640 (Sigma, Italy) supplemented with 10 % fetal calf serum (Celbio, Italy), 2 mM L-glutamine, and a 1 % streptomycin/penicillin antibiotic mixture (Sigma, Italy) under standard culture conditions (95 % O_2/5 % CO_2 at 37 °C in a humidified atmosphere). Cell survival following exposure to platinum complexes was evaluated using the 3-(4,5-dimethylthiazol-2-yl)-2,5-diphenyltetrazolium bromide (MTT) assay, based on the reduction of MTT by living cells [28]. Briefly, 1×10^3 cells per well were plated onto 96-well sterile plates and allowed to attach and grow for 24 h. **PtL1** was dissolved in ethanol to obtain a 10 mM stock solution that was diluted with complete medium for cell treatment. The final range of platinum concentrations was 0.1–5 μM and the co-solvent concentration never exceeded 0.1 % v/v; the effects of this ethanol concentration were tested on each cell line and were found to be negligible. In the case of **Pt(L1)$_2$**, concentrations greater than 2 μM could not be achieved, owing to the low solubility of the complex. After 3 days, MTT was added to each well (final concentration 0.4 mg mL^{-1}) and the plates were incubated for 3 h at 37 °C. Cell viability was determined by measuring the absorbance ($\lambda = 570$ nm) in individual wells, using a universal microplate reader (Bio-Tek Instruments, Winooski, VT, USA); survival fractions were calculated on the basis of the ratio between the absorbances obtained at each platinum complex concentration and the absorbance measured in control cells following subtraction of the mean background absorbance, and were plotted as a function of platinum complex concentrations. Whenever possible, a complete dose–response curve was obtained for each compound and nonlinear regression analysis of dose–response data was performed using GraphPad Prism 4 (GraphPad Software, La Jolla, CA, USA) to estimate the drug concentrations inhibiting tumor cell growth by 50 % (IC_{50}), Differences in cytotoxicity were statistically evaluated using one-way analysis of variance with Bonferroni's post hoc test.

DNA interaction

The plasmid DNA used for gel electrophoresis experiments was ϕX174 plasmid DNA (Promega). DNA interaction was evaluated by monitoring the mobility of the supercoiled plasmid DNA (covalently closed circular) and open circular DNA, as previously described [29]. Each reaction mixture was prepared by adding 6 μL water, 2 μL (200 ng) supercoiled DNA, 2 μL 100 mM stock Na_2HPO_4/HCl pH 7.2 buffer solution, and 10 μL of the solution of the complex. The final reaction volume was 20 μL, the final buffer concentration was 10 mM, and the final metal concentration ranged from 0.1 to 100 μM, corresponding to an input molar ratio of platinum to nucleotide (r_i) of 0.03–3.33. Samples were typically incubated for 24 h at 37 °C. After incubation, 4 μL DNA loading buffer (0.25 % bromophenol blue, 0.25 % xylene, in the dark cyanol, 30 % glycerol in water, Applichem) was added to each tube and the sample was loaded onto a 0.8 % agarose gel in 40 mM tris(hydroxymethyl)aminomethane, 20 mM acetic acid, and 1 mM EDTA pH 8.0 (TAE buffer). Controls consisting of nonincubated plasmid and plasmid incubated with dimethyl sulfoxide were loaded in each run. The electrophoresis was conducted for 3.5 h at 90 V.

In the case of the studies with chloroquine, the reaction mixture was prepared as previously described but with final metal complex concentrations of 1 μM ($r_i = 0.033$) and 10 μM ($r_i = 0.33$). The samples were incubated for 24 h at 37 °C. After the addition of DNA loading buffer, the samples were loaded onto a 0.8 % agarose gel in TAE buffer, and the electrophoresis run was performed for 16 h at 20 V in TAE buffer containing chloroquine at a concentration of 1.25 μg mL^{-1} (in order to resolve DNA topoisomers). The gels were then stained with TAE buffer containing ethidium bromide (0.5 μg mL^{-1}). Bands were visualized under UV light and images were captured using an AlphaImager EP gel documentation system (Alpha

Innotech). All samples in each figure were obtained from the same run; three to five independent replications were performed for each experiment.

G-quadruplex

$AG_3(TTAGGG)_3$ (22AG) 5′-end-radiolabeled with ^{32}P was mixed with 100 μM nonradiolabeled material in 50 mM $NaClO_4$ for 5 min at 90 °C and allowed to reach room temperature in 2 h to induce the formation of the quadruplex structure. It was then incubated with 100-300 μM platinum complex. The reactions were run for 16 h at 37 °C. The platinated oligonucleotides were separated using 20 % polyacrylamide denaturing gel electrophoresis and then isolated from the gels. The platination sites were determined by means of biochemical methods using 3′-exonuclease digestion [30–32]. All products of platination were quantified using a Storm 960 phosphorimager (Molecular Dynamics, GE Healthcare, France) and the ImageQuant software program. UV melting was measured at 2 μM oligonucleotide concentration by following the absorbance at 295 nm as function of increasing or decreasing temperature [33]. Experiments were performed in triplicate.

Results and discussion

Solution behavior and lipophilicity

The solution behavior of **PtL1**, **PtL2**, and **PtL3** was studied in 1 mM aqueous solutions containing 35 % ethanol (in order to have similar solubility conditions for all complexes) at 37 °C by means of HPLC–MS. All the complexes underwent hydrolysis (a molecule of water replaced a coordinated chloride), but with moderately different half-times $t_{½}$ (obtained with the method of initial rate): 1.0 h for **PtL1**, 1.9 h for **PtL3**, 2.9 h for **PtL2**. As expected, **PtL1**, the least bulky complex, has the fastest kinetics; surprisingly, the isomers **PtL2** and **PtL3** differed from each other in terms of $t_{½}$, but by 1 h only. Owing to the low solubility of **Pt(L1)$_2$**, its behavior was studied in a 0.1 mM solution containing 60 % ethanol, resulting in a hydrolysis $t_{½}$ of 9.9 h (under identical conditions, for example, $t_{½}$ for **PtL3** was 8.1 h). Importantly, HPLC chromatograms and MS spectra did not show the presence of the free ligand during solvolysis.

The lipophilicity of all the platinum complexes was evaluated by means of reversed-phase HPLC. Since the reversed-phase HPLC capacity factor ($k' = (t_R - t_0)/t_0$, where t_0 is the retention time for an unretained compound and t_R is the retention time of the species analyzed) is due to partitioning between (polar) mobile and (apolar) stationary phases, this parameter is related to the hydrophobicity of the compound. In this work, $\log k'_{80}$ values of the compounds (measured at 80 % methanol eluent) were used (the lower the $\log k'_{80}$, the higher the hydrophilicity; Table 1). As expected, **PtL1** was found to be less lipophilic than **PtL2** and **PtL3**, and less hydrophilic than cisplatin. **Pt(L1)$_2$**, **PtL2**, and **PtL3** exhibited similar retention behavior and, hence, similar lipophilicity. Since cellular platinum uptake is exponentially related to the lipophilicity of the complexes [34, 35], it can be assumed that **Pt(L1)$_2$**, **PtL2**, and **PtL3** have a similar uptake, which is higher than that of **PtL1**, which in turn is superior to that of both cisplatin and oxaliplatin.

Cytotoxicity tests

PtL1 and **Pt(L1)$_2$** were tested on three different cell lines (i.e., A2780 ovarian carcinoma and its cisplatin-resistant form A2780Cp8, and colon adenocarcinoma HCT116) following 72 h exposure. Cytotoxicity is expressed as IC_{50} (Table 1). The IC_{50} for **Pt(L1)$_2$** could not be determined because of its low solubility. The data were compared with those obtained for cisplatin, oxaliplatin, **PtL2**, and **PtL3** determined under identical experimental conditions [18]. Since it had been previously verified (via ^{195}Pt NMR spectroscopy) that DABN complexes undergo rapid degradation when dissolved in dimethyl sulfoxide [18], the complexes were tested with ethanol as a co-solvent. The final ethanol concentration in culture medium never exceeded 0.1 % v/v; the effects of this ethanol concentration in drug-free medium were tested separately and were found to be negligible (not shown).

PtL1, **PtL2**, and **PtL3** appear to be equally potent with regard to ovarian cells (including the cisplatin-resistant variant) and colorectal cells; indeed, their performance with regard to HCT116 cells was almost as good as that of oxaliplatin, which has been in clinical use for treatment of colorectal cancer for more than a decade, whereas cisplatin was significantly less potent against HCT116 cells than against A2780 cells, confirming the intrinsic resistance of colon cancer to cisplatin-based therapies [27]. Possibly, the presence of aminonaphthalene rings mimics the effects of the cyclohexanediamine moiety in oxaliplatin and might thus enable **PtL1**, **PtL2**, and **PtL3** to target tumors that respond poorly to cisplatin. These complexes also showed a lower resistance factor (i.e., the ratio between the IC_{50} values for cisplatin-resistant A2780Cp8 and A2780 cells) as compared with cisplatin, indicating their ability to circumvent acquired as well as intrinsic cisplatin resistance.

As previously noted, the *S* isomer, **PtL3**, was slightly more active than the *R* counterpart, **PtL2**. A similar relationship between cytotoxic activity and chirality has been

Table 1 Half-maximal inhibitory concentrations (IC_{50}) and $\log k'_{80}$ values of the compounds investigated (mean ± standard error of four or five determinations)

Compounds	IC_{50} (μM) A2780	IC_{50} (μM) A2780Cp8	Resistance factor	IC_{50} (μM) HCT116	$\log k'_{80}$
Cisplatin[a]	1.15 ± 0.09[c]	14.99 ± 0.44[e]	13.0	10.98 ± 1.9[e]	−0.54
Oxaliplatin[a]	0.63 ± 0.11	0.55 ± 0.11	0.87	0.66 ± 0.03	−0.41
PtL1	0.44 ± 0.12[d]	2.49 ± 0.45	5.66	1.48 ± 0.07	−0.34
Pt(L1)$_2$	ND[b]	ND[b]	ND[b]	ND[b]	−0.13
PtL2[a]	1.36 ± 0.3	1.58 ± 0.51	1.16	0.98 ± 0.05	−0.16
PtL3[a]	1.15 ± 0.11	1.27 ± 0.35	1.10	1.61 ± 0.14	−0.16

See Fig. 1 for the structures of the complexes

ND not determined

[a] Data from [18]

[b] See the text

[c] $p < 0.05$ versus oxaliplatin

[d] $p < 0.05$ versus **PtL2**

[e] $p < 0.001$ versus all other complexes

observed for [Pt(ampyr)(cbdca)] (ampyr is aminomethylpyrrolidine and cbdca is cyclobutanedicarboxylate) complexes, where the *R* isomer is less toxic than the *S* isomer. Bloemink et al. [36] studied the interaction of these isomers with short oligonucleotides and showed that both form 1,2-intrastrand cross-linking adducts similarly to cisplatin. However, relative to the *S* isomer, the adduct of the *R* isomer has more steric hindrance between the bulky pyrrolidine ring and the DNA fragments, and this difference may be responsible for the reduced toxicity of the *R* isomer [36]. The relationship between chirality and biological activity is not well understood, but this structural feature may be relevant in some cases: oxaliplatin and lobaplatin are examples of "chiral platinum drugs" which are in clinical use. In the case of oxaliplatin, in vitro cytotoxicity assays and animal studies showed that the complex with the (1*R*,2*R*)-cyclohexanediamine ligand has the highest potential as an antitumor agent [37]. Also in the case of [$PtCl_2$(en*)] (where en* is substituted ethane-1,2-diamines containing one and two chiral carbon centers), a substantial difference in mutagenicity between the *R*,*R*, *S*,*S*, and *R*,*S* isomers was observed [38].

As mentioned earlier, no IC_{50} values could be obtained for **Pt(L1)$_2$**, owing to its low solubility under the experimental conditions adopted. However, the survival fractions following exposure to equimolar concentrations (1 μM) of **PtL1**, **PtL2**, **PtL3**, and **Pt(L1)$_2$** were compared (see Fig. S1). On the basis of these data, **Pt(L1)$_2$** may be considered to be less effective than **PtL1**, but almost comparable to **PtL2** and **PtL3**. Thus, the observed solvolytic behavior and lipophilicity of the complexes do not seem to affect cytotoxicity, suggesting that differences in $t_{½}$ and $\log k'_{80}$ of the compounds studied are probably smoothed during the 72-h cytotoxicity experiments.

Interaction of platinum complexes with supercoiled DNA

The effect of the interaction of **PtL1**, **PtL2**, and **PtL3** as well as their ligands **L1**, **L2**, and **L3**, and **Pt(L1)$_2$** with supercoiled DNA was determined by their ability to modify the electrophoretic mobility of the covalently closed circular (form I) and open circular (open circular, form II) forms of ϕX174 plasmid DNA. For platinum complexes, it has been reported that at increasing molar ratios of platinum bound per nucleotide (r_b), the rate of migration of the covalently closed circular DNA form decreases until it co-migrates with the open circular DNA form, so r_b at the coalescence point corresponds to the amount of platinum needed for complete removal of all supercoils from DNA [29, 39]. The three ligands **L1**, **L2**, and **L3** did not induce any changes in the rate of migration of either DNA form, as compared with the control (untreated) plasmid. However, when the same experiments were performed with the platinum complexes, all of them induced a decrease in the mobility of the covalently closed circular DNA forms, leading to co-migration of the covalently closed circular and open circular DNA forms, albeit at different Pt(II)-to-DNA ratios (Fig. 2).

These studies were also used to assess the DNA unwinding angle, ϕ, induced by the Pt(II) complexes; it can be calculated from the equation $\phi = 18\sigma/r_b(c)$, where σ is the superhelical density of the plasmid and $r_b(c)$ is the molar ratio of platinum bound per nucleotide at the coalescence point [40]. For **PtL2** and **PtL3**, $r_b(c)$ values of 0.1 and 0.33, corresponding to concentrations of 3 and 10 μM, respectively, were found. Under the actual experimental conditions ($\sigma = -0.116$, superhelical density determined assuming the value of $\phi = 13°$ for cisplatin), the DNA

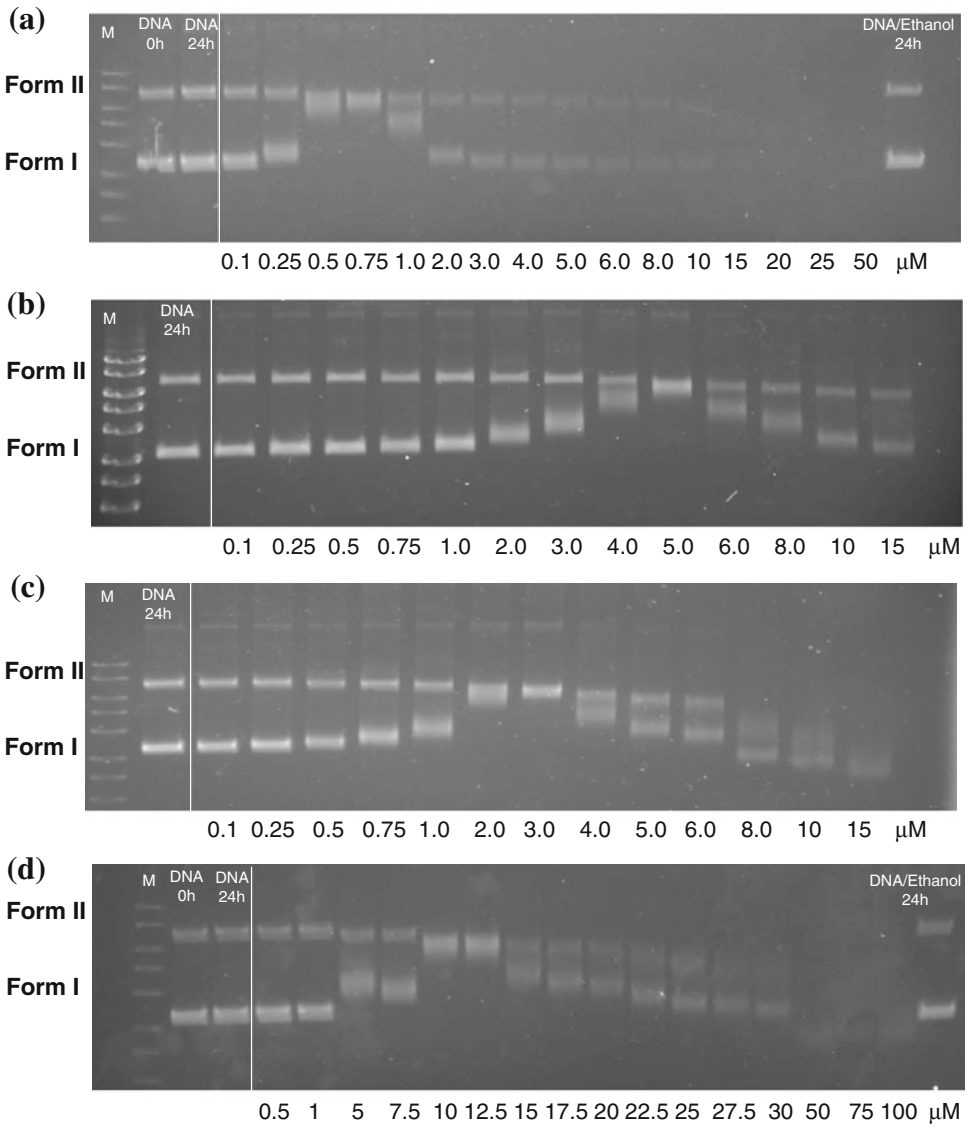

Fig. 2 Interaction between supercoiled plasmid DNA and **a PtL1**, **b Pt(L1)$_2$**, **c PtL2**, and **d PtL3** after 24 h of incubation at 37 °C in phosphate buffer (pH 7.2). Form I and form II are the covalently closed circular and open circular forms of DNA, respectively

unwinding angles were 20.9° and 6.3° for **PtL2** and **PtL3**, respectively. Taking into account the ϕ value obtained for cisplatin (13°) [41–43] and the increase, albeit modest, observed for **PtL2**, we can propose a different mode of interaction with plasmid DNA. For the complex containing the *R* isomer, intercalative binding may contribute, even though this type of interaction seems to play a minor role. For **Pt(L1)$_2$**, the unwinding angle was similar to that calculated for cisplatin (12.5° vs 13°); arguably, the two naphthalene moieties around the platinum center hinder each other, which limits DNA intercalation and leaves alkylation as the predominant mechanism for interaction. In contrast, in the case of the 2-aminonaphthalene complex, **PtL1**, the coalescence point occurred at a very low concentration of the metal complex (0.75 µM), corresponding to a very high ϕ value (83.5°). In this case, the interaction with DNA probably involves a combination of platination and intercalation, conceivably due to the presence of a single aromatic ligand.

The combination of intercalation and platination effects was further verified in the presence of chloroquine. In these studies, ligands **L1**, **L2**, and **L3** and their corresponding Pt(II) complexes were incubated with DNA at 37 °C for 24 h, and the different mixtures were subsequently analyzed by agarose gel electrophoresis in the presence of chloroquine (Fig. 3).

Chloroquine induces positive supercoiling of plasmid DNA, and promotes the resolution of topoisomeric forms of the plasmid: the slowest moving band of each lane corresponds to the open circular form, whereas the other bands of each lane correspond to covalently closed circular forms or topoisomers. The experiments showed that there

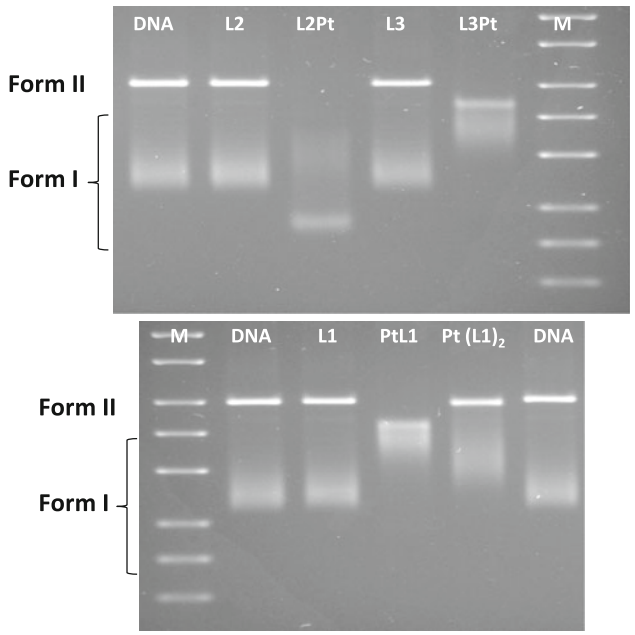

Fig. 3 Resolution of DNA topoisomers of ϕX174 phage incubated with ligand **L1** and the corresponding Pt(II) complexes—**PtL1** and **Pt(L1)$_2$**—at a molar ratio of added platinum complex per nucleotide (r_i) of 0.033 (1 μM) (*bottom*), and ligands **L2** and **L3** ligands and the corresponding Pt(II) complexes—**PtL2** and **PtL3**—at $r_i = 0.33$ (10 μM) (*top*). The experimental conditions were as follows: incubation time 24 h at 37 °C in phosphate buffer (pH 7.2), after agarose gel electrophoresis with chloroquine (1.25 μg mL^{-1})

were no significant differences in the mobility of DNA topoisomer bands in the case of free ligands, when compared with control DNA in the presence of chloroquine, as expected. A slower migration was observed for **PtL1** and **Pt(L1)$_2$**, probably owing to the presence of Pt–DNA adducts that were not displaced by chloroquine. Notably, **PtL1** induced a greater delay than **Pt(L1)$_2$** in the mobility of the topoisomers, relative to the control. This finding suggests that **PtL1** acts as a strong intercalator and causes a negative twist in the structure of supercoiled DNA, with chloroquine being unable to cause its displacement from the DNA double helix.

For **PtL2**, the migration rate was markedly lower than that of control plasmid, but was reached at higher platinum-to-nucleotide ratios with respect to those used in the experiments with **PtL1** and **Pt(L1)$_2$**. In the case of **PtL3**, the delay in the mobility was less important, pointing out, once again, the different general biological behavior of the two isomers. However, in both cases the complete dissociation of DNA complexes was not produced even in the presence of an excess of chloroquine.

Taken together, the DNA interaction data obtained for the four complexes show that these compounds have different DNA-binding abilities, with a more evident contribution of the intercalative binding mode in the case of **PtL1**.

Interaction of platinum complexes with G-quadruplexes

Recently, the enantiomeric complexes **PtL2** and **PtL3** were tested for their ability to bind human telomeric sequences folded into a G-quadruplex structure [18]. Similar experiments have been performed in the present study, to compare the behavior of **PtL2** and **PtL3** with that of **PtL1** and **Pt(L1)$_2$**.

For this reason, $AG_3(TTAGGG)_3$, indicated as 22AG (Fig. 4, left), 5′-end-labeled with ^{32}P, was allowed to fold into a G-quadruplex structure in the presence of 50 mM $NaClO_4$, and subsequently incubated overnight with 1–3 equiv of each of the platinum complexes tested. Platination products were then separated by gel electrophoresis (Fig. 4, right) and isolated. The different migration rates of the products depend on the number of platinum complexes bound to 22AG; therefore, a slower migration product is supposed to contain at least one platinum complex. Platinum binding sites in the various products were determined by exonuclease digestion.

Incubation of the telomeric G-quadruplexes with **PtL1** was found to yield new products that migrate through the gel at a lower rate (product 2) as already found for **PtL2** and **PtL3**, but also at a faster rate (product 1) than 22AG under control conditions, indicating that the G-quadruplex structure of 22AG was platinated. The faster migrating product is indicative of a still structured form of the telomeric sequence, probably a G-quadruplex structure stable enough to resist the denaturing conditions. These stable DNA structures have already been depicted for G-quadruplexes cross-linked by cisplatin [30] or platinated by a Pt–G-quadruplex ligand (Pt– mono-*para*-quinacridine) that is able to stabilize the structure thanks to the stacking effect of the mono-*para*-quinacridine [32]. In contrast, **Pt(L1)$_2$** does not platinate 22AG.

The isomeric complexes **PtL2** and **PtL3** have already been shown to platinate G-quadruplexes with different efficiency, whereby the *R* isomer yields a smaller amount of platinated products. For this reason, the stereochemical arrangement of the organic ligand has been proposed to play an important role in determining the interaction between the platinum moiety and nucleobases [18]. The role of the three-dimensional arrangement is further supported by the results obtained in the present study as regards the behavior of **PtL1**. Indeed, the yield of G-quadruplex platination is greater for **PtL1** (which contains only one naphthalene group) than for **PtL2**, and **PtL3** (containing two linked naphthalenes). In the case of **Pt(L1)$_2$** (containing two independent naphthalenes), it is possible to hypothesize that the presence of two unconstrained naphthalene groups may prevent platination of G-quadruplex structures, probably by steric hindrance;

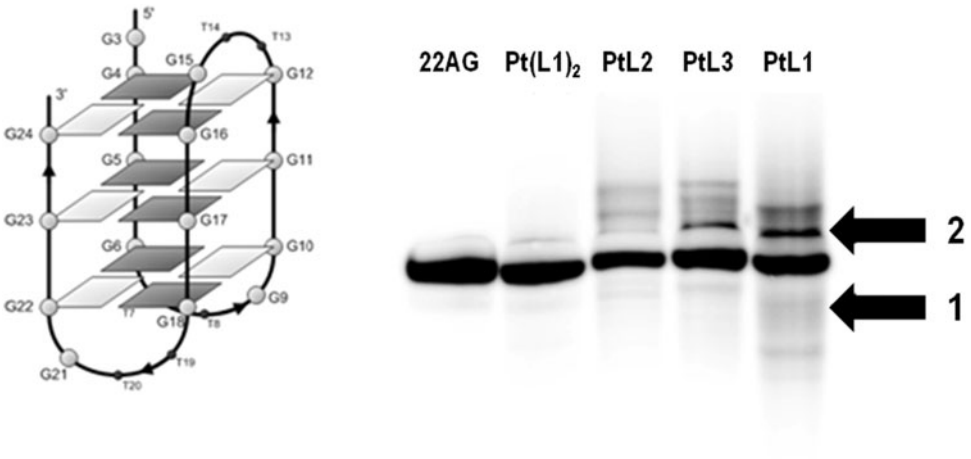

Fig. 4 *Left*: Antiparallel G-quadruplex structure of telomeric sequence $AG_3(TTAGGG)_3$ (*22AG*). *Right*: Electrophoresis gel after platination of the quadruplex structure of 22AG by the platinum complexes (from *left* to *right*): no drug, **Pt(L1)$_2$**, **PtL2**, **PtL3**, and **PtL1**

however, the low solubility of **Pt(L1)$_2$** may play a role in this experiment.

The platination sites identified for **PtL1**, **PtL2**, and **PtL3** are specific of the platination of telomeric G-quadruplex structure, since only the adenines of the loops (A7, A13, or A19) and/or one guanine of the 5′ external G-quartet of the antiparallel structure (G10) are platinated.

Previous results obtained with **PtL2** and **PtL3** indicate that the major binding sites on the G-quadruplex structure of 22AG are G10 and A19 [18]; in contrast, **PtL1** preferentially binds A13 for the faster migrating product 1 and A7, A13, or A19 for the slower migrating product 2 from Fig. 4 (see Fig. S2). Comparative platination profiles of **PtL1**, **PtL2**, and **PtL3** suggest that access to platination sites also depends on the number of naphthalene groups. **PtL1** is able to bind to two more platinum binding sites than **PtL2** and **PtL3**, probably owing to less steric hindrance (only one naphthalene moiety): these involve two adenines located in the loops (A7 and A13). Since A7 is the most accessible platination site of the antiparallel G-quadruplex structure as calculated by molecular modeling [31] and corresponds also to the major platination site of terpyridine-Pt [44], which is not able to stabilize the G-quadruplex structure, it can be concluded that this platination site could result from a nonspecific interaction of **PtL1** with the G-quadruplex structure. However, the other binding site of **PtL1** is A13, which corresponds to the major platination site of tolylterpyridine–Pt, which is a strong binder of G-quadruplex [44], and it can be concluded that this platination event could occur after G-quartet interaction. This result is reinforced by the data showing that the A13 platinum adduct of the G-quadruplex structure is highly stable since it migrated faster on gel electrophoresis even in denaturing conditions (product 1). These results suggest that **PtL1** is a stronger binder of telomeric G-quadruplex structure than **PtL2** and **PtL3**. It can stack on one external G-quartet and platinate the adenine residue close to it, cross-linking consequently irreversibly the G-quadruplex structure. The platination binding sites suggest that **PtL1**, **PtL2**, and **PtL3** do not interact similarly with the external G-quartet.

Moreover, the affinity of **PtL1** for these structures was confirmed by using melting temperature experiments and monitoring the optical density at 295 nm, which allows detection of the folding and unfolding of the structure as a function of temperature; its behavior was compared with that of **Pt(L1)$_2$**, which does not cross-link G-quadruplexes. **Pt(L1)$_2$** caused a decrease in the optical density of the G-quadruplex structure of 22AG at increasing temperatures that is characteristic of a dynamic state of the structure, analogous to the one observed without any ligand. In contrast, in the presence of **PtL1** (or **PtL2** or **PtL3**, as described in [18]), no decrease in optical density was observed under identical experimental conditions, indicating that interaction with the complexes has trapped the G-quadruplex in a folded state that cannot be reversed by high temperatures (Fig. S3). Therefore, **PtL1** shows a more evident intercalative binding mode in double-stranded DNA and a more efficient stacking followed by cross-linking of the G-quadruplex structures compared with **PtL2** and **PtL3**. These results indicate that **PtL1** did not show any structural preference for double-stranded or G-quadruplex DNA, as found for **PtL3** [18].

Conclusions

Two new Pt(II) complexes containing a 2-aminonaphthalene ligand—**PtL1** and **Pt(L1)$_2$**— have been synthesized and fully characterized. The cytotoxicity with regard to one colorectal (HCT116) and two ovarian (A2780 and A2780Cp8) carcinoma cell lines and their DNA- and

G-quadruplex-binding properties have been investigated. The cytotoxicity of the complexes is comparable to, and in some cases even better than, that of cisplatin, and rather resembles that of oxaliplatin, as no significant differences in response were observed in cells with acquired resistance to cisplatin (A2780Cp8) or in HCT116 colorectal adenocarcinoma cells, which intrinsically respond poorly to cisplatin owing to defective mismatch repair activity [26], as compared with cisplatin-sensitive A2780 cells.

The observed solvolytic behavior (all the complexes underwent cisplatin-like hydrolysis without loss of the aromatic amines, with half-times ranging from approximately 1 h to approximately 3 h) and the absence of an evident relationship between lipophilicity and cytotoxicity seem to suggest that these experimental features are probably smoothed during the 72-h experiments and do not influence greatly the IC_{50} values. Electrophoresis tests demonstrated that different kinds of interactions with DNA can be involved in the mode of action of these complexes, with intercalation being strongly implicated for **PtL1**. All these considerations suggest that the differences in cytotoxicity may be related to different interaction with DNA, as well as with other possible intracellular targets.

PtL1 is also able to stabilize telomeric G-quadruplex structures and to cross-link them irreversibly thanks to the platination of an adenine located in the loop. However, its lack of specific recognition of G-quartet structures prevents it from being considered as a promising G-quadruplex binder; in contrast, the experimental data suggest that it may be regarded as a good DNA intercalator.

Acknowledgments The research was conducted within the framework of the European Cooperation COST CM1105 (Functional Metal Complexes That Bind to Biomolecules) and Consorzio Interuniversitario di Ricerca in Chimica dei Metalli nei Sistemi Biologici (CIRCMSB, Bari, Italy).

References

1. Bischoff G, Hoffmann S (1996) Curr Med Chem 9:321–348
2. Brabec V (2002) Prog Nucleic Acid Res Mol Biol 71:1–68
3. Erkkila KE, Odom DT, Barton JK (1999) Chem Rev 99:2777–2795
4. Zeglis BM, Pierre VC, Barton JK (2007) J Chem Soc Chem Commun 4565–4579
5. Georgiades SN, Karim NHA, Suntharalingam K, Vilar R (2010) Angew Chem Int Ed 49:4020–4034
6. Natile G, Cannito F (2009) In: Hadjiliadis N, Sletten E (eds) Metal complex–DNA interactions. Wiley-Blackwell, Chichester, pp 135–173
7. Rabik CA, Dolan ME (2007) Cancer Treat Rev 33:9–23
8. Ourliac-Garnier I, Charif R, Bombard S (2009) In: Hadjiliadis N, Sletten E (eds) Metal complex–DNA interactions, Wiley-Blackwell, Chichester, pp 209–234
9. Palm W, de Lange T (2008) Annu Rev Genet 42:301–334
10. Burge S, Parkinson GN, Hazel P, Todd AK, Neidle S (2006) Nucleic Acids Res 34:5402–5415
11. Neidle S (2009) Curr Opin Struct Biol 19:239–250
12. Harley CB, Futcher AB, Greider CW (1990) Nature 345:458–460
13. Zahler AM, Williamson JR, Cech TR (1991) Nature 350:718–720
14. Riou JF, Guittat L, Mailliet P, Laoui A, Renou E, Petitgenet O, Megnin-Chanet F, Helene C, Mergny JL (2002) Proc Natl Acad Sci USA 99:2672–2677
15. Gomez D, Wenner T, Brassart B, Douarre C, O'Donohue MF, El Khoury V, Shin-Ya K, Morjani H, Trentesaux C, Riou JF (2006) J Biol Chem 281:38721–38729
16. Tahara H, Shin-Ya K, Seimiya H, Yamada H, Tsuruo T, Ide T (2006) Oncogene 25:1955–1966
17. Rodriguez R, Miller KM, Forment JV, Bradshaw CR, Nikan M, Britton S, Oelschlaegel T, Xhemalce B, Balasubramanian S, Jackson SP (2012) Nat Chem Biol 8:301–310
18. Bombard S, Gariboldi MB, Monti E, Gabano E, Gaviglio L, Ravera M, Osella D (2010) J Biol Inorg Chem 15:841–850
19. Abrams MJ, Giandomenico CM, Vollano JF, Schwartz DA (1987) Inorg Chim Acta 131:3–4
20. Giandomenico CM, Abrams MJ, Murrer BA, Vollano JF, Rheinheimer MI, Wyer SB, Bossard GE, Higgins JD (1995) Inorg Chem 34:1015–1021
21. Monti E, Gariboldi MB, Ravizza R, Molteni R, Sparnacci K, Laus M, Gabano E, Ravera M, Osella D (2009) Inorg Chim Acta 362:4099–4109
22. Miller B, Wild S, Zorbas H, Beck W (1999) Inorg Chim Acta 290:237–246
23. Platts JA, Oldfield SP, Reif MM, Palmucci A, Gabano E, Osella D (2006) J Inorg Biochem 100:1199–1207
24. Heudi O, Mercier-Jobard S, Cailleux A, Allain P (1999) Biopharm Drug Dispos 20:107–116
25. Papadopoulos N, Nicolaides NC, Wei YF, Ruben SM, Carter KC, Rosen CA, Haseltine WA, Fleischmann RD, Fraser CM, Adams MD, Venter JC, Hamilton SR, Peterson GM, Watson P, Lynch HT, Peltomaki P, Mecklin JP, de la Chapelle A, Kinzler KW, Vogelstein B (1994) Science 263:1625–1629
26. Umar A, Boyer JC, Thomas DC, Nguyen DC, Risinger JI, Boyd J, Ionov Y, Perucho M, Kunkel TA (1994) J Biol Chem 269:14367–14370
27. Cvitkovic E (1998) Br J Cancer 77(Suppl 4):8–11
28. Alley MC, Scudiero DA, Monks A, Hursey ML, Czerwinski MJ, Fine DL, Abbott BJ, Mayo JG, Shoemaker RH, Boyd MR (1988) Cancer Res 48:589–601
29. Francisco C, Gama S, Mendes F, Marques F, Cordeiro dos Santos I, Paulo A, Santos I, Coimbra J, Gabano E, Ravera M (2011) Dalton Trans 40:5781–5792
30. Redon S, Bombard S, Elizondo-Riojas MA, Chottard JC (2003) Nucleic Acids Res 31:1605–1613
31. Ourliac-Garnier I, Elizondo-Riojas MA, Redon S, Farrell NP, Bombard S (2005) Biochemistry 44:10620–10634
32. Bertrand H, Bombard S, Monchaud D, Teulade-Fichou MP (2007) J Biol Inorg Chem 12:1003–1014
33. Mergny JL, Phan AT, Lacroix L (1998) FEBS Lett 435:74–78
34. Ghezzi AR, Aceto M, Cassino C, Gabano E, Osella D (2004) J Inorg Biochem 98:73–78
35. Platts JA, Hibbs DE, Hambley TW, Hall MD (2001) J Med Chem 44:472–474
36. Bloemink MJ, Pérez JM, Heetebrij RJ, Reedijk J (1999) J Biol Inorg Chem 4:554–567
37. Hambley TW (1997) Coord Chem Rev 166:181–223
38. Gust R, Beck W, Jaouen G, Schönenberger H (2009) Coord Chem Rev 2009:2760–2779
39. Keck MV, Lippard SJ (1992) J Am Chem Soc 114:3386–3390
40. Cohen G, Bauer W, Barton J, Lippard SJ (1979) Science 203:1014–1016

41. Scovell WM, Collart F (1985) Nucleic Acids Res 13:2881–2895
42. Bellon SF, Coleman JH, Lippard SJ (1991) Biochemistry 30:8026–8035
43. Moradell S, Lorenzo J, Rovira A, Robillard MS, Avilés FX, Moreno V, de Llorens R, Martinez MA, Reedijk J, Llobet A (2003) J Inorg Biochem 96:493–502
44. Bertrand H, Bombard S, Monchaud D, Talbot E, Guédin A, Mergny JL, Grünert R, Bednarski PJ, Teulade-Fichou MP (2009) Org Biomol Chem 7:2864–2871